HHS Public Access

Author manuscript

Ophthalmol Retina. Author manuscript; available in PMC 2022 December 14.

Published in final edited form as:

Ophthalmol Retina. 2021 August ; 5(8): 730–742. doi:10.1016/j.oret.2020.11.006.

Stages of drusen-associated atrophy in age-related macular degeneration visible via histologically validated fundus autofluorescence

Ling Chen, MD PhD[1,2], **Jeffrey D. Messinger, DC**[1], **Daniela Ferrara, MD PhD**[3], **K. Bailey Freund, MD**[4,5,6,7], **Christine A. Curcio, PhD**[1,*]

[1]Department of Ophthalmology and Visual Sciences, University of Alabama at Birmingham School of Medicine, Birmingham Alabama, USA

[2]The First Affiliated Hospital of Chongqing Medical University, Chongqing Key Laboratory of Ophthalmology, and Chongqing Eye Institute, Chongqing, China.

[3]Genentech, South San Francisco, CA, USA

[4]Vitreous Retina Macula Consultants of New York, New York, NY, USA

[5]LuEsther T. Mertz Retinal Research Center, Manhattan Eye, Ear and Throat Hospital, New York, NY, USA

[6]Department of Ophthalmology, New York University School of Medicine, New York, NY, USA

[7]Columbia University College of Physicians and Surgeons, Harkness Eye Institute, New York, NY, USA

Abstract

Purpose: To determine histologic correlates for defined stages of drusen-associated atrophy observed with multimodal imaging including fundus autofluorescence (FAF) and color fundus photography (CFP) of eyes with advanced age-related macular degeneration (AMD).

Design: Case study and clinicopathologic correlation.

Subject: A white woman in whom AMD findings of inactive subretinal fibrosis (right eye) and untreated non-exudative type 1 macular neovascularization (left eye) were followed for 9 years before death at age 90 years.

Methods: Eyes preserved 6.25 hours after death were post-fixed in osmium tannic acid paraphenylenediamine and prepared for sub-micrometer epoxy resin sections (n=115, 90 in right and left eyes, respectively), with 19 aligned to clinical OCT B-scans. Drusen visible by CFP at the last visit were assigned to 4 stages of *in vivo* FAF: Stage 1, isoFAF, no obvious FAF alteration;

[*]**Corresponding Address:** Christine A. Curcio, PhD; Department of Ophthalmology and Visual Sciences; EyeSight Foundation of Alabama Vision Research Laboratories; 1670 University Boulevard Room 360; University of Alabama School of Medicine; Birmingham AL 35294-0099; christinecurcio@uabmc.edu.

Financial disclosure:
KBF is a consultant to Genentech, Bayer, Zeiss, Heidelberg Engineering, Allergan, and Novartis and receives research funds from Genentech/ Hoffman LaRoche. CAC receives research funds from Genentech/ Hoffman LaRoche and Heidelberg Engineering and is a stockholder of MacRegen Inc. DF is an employee of Genentech and has stock/stock options of Hoffman LaRoche.

Stage 2, mildly uniform hyperFAF; Stage 3, a ring of hyperFAF around a center of hypoFAF; and Stage 4, uniform hypoFAF.

Main outcome measures: Light microscopic morphology at known FAF stages, including druse size, druse contents and changes in overlying retinal pigment epithelium (RPE), photoreceptors and external limiting membrane (ELM).

Results: Histology of 166 drusen demonstrated that stage 1 iso-FAF drusen were visible in CFP. HyperFAF in Stage 2 corresponded to short photoreceptors and complete coverage by RPE. HypoFAF in Stage 3 and 4 corresponded to different extents of RPE atrophy (RPE gap and no RPE, respectively). Of stage 4 drusen, 67% have no ONL and an undetectable ELM. Stage 4 includes a high proportion of refractile drusen (82%) with many calcific nodules, visible in CFP.

Conclusion: This represents the first direct clinicopathologic correlation for FAF imaging of drusen-associated atrophy. Our data support 4 FAF stages of drusen-associated atrophy. Stage 2 is the earliest detected stage in which loss of screening by photoreceptor photopigment contributes to uniform hyperFAF. Stages 3 and 4 are consistent with incomplete RPE and outer retinal atrophy (iRORA) as defined by the Classification of Atrophy Meetings group. Loss of RPE, ONL and ELM in Stage 4 indicates that atrophy can begin over individual drusen. Our findings will help the identification of new therapeutic approaches and clinical study endpoints.

Précis:

Histology of eyes with clinical multimodal imaging reveals stages of incomplete retinal pigment epithelium and outer retinal atrophy over drusen. Photoreceptor degeneration contributes to uniform hyperautofluorescence. Atrophy contributes to hypoautofluorescence over drusen centers, then entireties.

Tweet

Histology of eyes with clinical multimodal imaging reveals stages of incomplete retinal pigment epithelium and outer retinal atrophy over drusen. Photoreceptor degeneration contributes to uniform hyperautofluorescence, a newly defined early stage.

Keywords

age-related macular degeneration; atrophy; drusen; drusen-associated atrophy; photoreceptors; retinal pigment epithelium; autofluorescence; lipofuscin; incomplete RPE and outer retinal atrophy (iRORA)

Introduction

Age-related macular degeneration (AMD), the main cause of central vision loss among older adults in industrialized countries, is not treatable for the majority of patients. The status of the retinal pigment epithelium (RPE), key cells in AMD progression, is visible clinically through fundus autofluorescence (FAF) imaging for retinal disease diagnosis and management.[1] Clinicopathologic correlation of eyes imaged with FAF during life can validate diagnostic technology with anatomic ground truth and probe disease pathogenesis. Herein we report such a case, to aid clinical FAF interpretation.

The major signal source for FAF is lipofuscin and melanolipofuscin (L/ML), long-lasting membrane-bounded organelles that accumulate in RPE cell bodies starting in childhood. Classic studies of histologic autofluorescence in human retina linked FAF to L/ML, and FAF topography to that of the overlying photoreceptors.[2, 3] Recent studies illustrated and quantified RPE morphology, topography, and autofluorescent organelle types in normal aged eyes and eyes with AMD,[4–8] and introduced several new concepts. Normal foveal and perifoveal RPE are dominated by ML and L, respectively. Rounded and stacked RPE cells can account for hyperFAF in AMD. Autofluorescence in individual RPE cells is overall lower with AMD despite focal L/ML aggregations of high intensity. These findings support L/ML as an important indicator of RPE health. L/ML may itself be physiologically benign, contrary to widespread opinion.[9]

Research using fundus reflectometry showed that FAF is also modulated by cells outside the RPE layer. For example, photopigment in the overlying photoreceptors absorb both incoming and outgoing light and thus reduce the intensity of FAF signal from RPE.[10] For this reason, patients undergoing quantitative FAF imaging are first exposed to a bright light to standardize the level of photopigment bleaching.[11] This finding has diagnostic utility, as it was then shown that prior photoreceptor damage abolishes this bleaching effect and causes hyperFAF[12]. Thus, FAF signals may also reveal photoreceptor status.

Drusen confer risk for progression to atrophy and neovascularization with very large odds ratios.[13] In 2000, rings of FAF around hypoFAF centers were attributed to individual drusen by Delori et al.[14] Recently, FAF rings were shown as one stage of a sequence: uniform hyperFAF, rings, and uniform hypoFAF. [15] These stages were linked to a hyporeflective core within drusen seen by OCT,[16] a progression indicator corresponding to calcific nodules.[16] FAF rings were also seen around cuticular drusen, [17] which are overall smaller than soft drusen. It is possible that an FAF ring could be caused by absence or effacement of RPE on the druse apex with thickened RPE around the druse base. However, shortening of photoreceptors over drusen could also contribute to hyperFAF. Direct evidence from histology is currently lacking.

Currently, the only imaging endpoint for geographic atrophy secondary to AMD recognized by the US Food and Drug Administration as an approvable endpoint is expansion of pre-existing macular atrophy. Prevention of atrophy requires specific imaging findings indicative of disease stages preceding its occurrence. An international clinical consensus group is seeking to standardize imaging biomarkers for this purpose.[18] A sequence of events visible in FAF was hinted at in our prior publications.[15, 16] Previous histologic analysis of drusen-associated atrophy in cases with clinical FAF examined only the atrophy, and not the preceding steps. [18]

To fill these knowledge gaps, we asked if defined stages of FAF signal can be associated with drusen in AMD, and further, whether this signal is modulated by photoreceptors along with RPE. We performed high-resolution histologic analysis of two eyes of one patient with AMD and FAF imaging at 4 different times during life. Data confirm the association of hypoFAF with calcification, reveal the participation of photoreceptor degeneration, and demonstrate loss of outer retinal layers atop every atrophic druse examined. Data also

validate the appropriateness of nomenclature and classification system proposed by the Classification of Atrophy Meeting group.

Methods

Compliance

Retrospective review of medical records and imaging data and the histopathology study were approved by the institutional review boards of the Manhattan Eye, Ear, and Throat Hospital/Northwell Health and the University of Alabama at Birmingham, respectively. All study components complied with the Health Insurance Portability and Accountability Act of 1996 and adhered to the tenets of the Declaration of Helsinki. Written informed consent was obtained from the patient.

Clinical course

Comprehensive ophthalmologic examination and multimodal imaging was performed during a 9-year follow-up of a woman of European descent who presented with AMD at age 79 years. Ocular history included cataract surgery in both eyes. Medical history included chronic obstructive pulmonary disease (COPD), gastric cancer, and hypercholesterolemia. There was a 57 pack-year history of smoking. The patient presented with inactive subretinal fibrosis in the right eye and non-exudative type 1 macular neovascularization (MNV) in the left eye, as reported previously.[19] Best-corrected visual acuity (BCVA) was 20/50 in the right eye and 20/25 in the left eye at baseline.

At the last registered clinical evaluation, the patient maintained inactive subretinal fibrosis and non-exudative type 1 MNV in the right and left eye, respectively. Color fundus photography (CFP, Figure 1A,D) and FAF (Figure 1B,E) images (λ_{ex} = 532 nm; Optos California, Dunfermline, Scotland, UK) showed soft and refractile drusen that mostly spare the central macula. FAF imaging showed different focal FAF changes in the macular area, such as mild hyperFAF, a ring of hyperFAF around a center of hypoFAF, and hypoFAF, corresponding to different stages of drusen-associated atrophy (Figure 1B,E). SD-OCT (Heidelberg Spectralis HRA+OCT, Heidelberg Engineering, Heidelberg, Germany) showed in the left eye an extensive shallow irregular retinal pigment epithelium (RPE) elevation (SIRE) that has been reported[19] and a small soft druse. In the right eye, SD-OCT showed a SIRE and two drusen with hyporeflective cores (Figure 1C,F). Visual acuity was 20/200 in the right eye and 20/30 in the left eye.

Drusen evaluation on clinical imaging

CFP and FAF (λ_{ex}: 535–585 nm; TRC-50IX fundus camera; Topcon, Tokyo, Japan) from different time points during follow-up were reviewed. FAF features and stages of drusen referenced to CFP at the same location and same timepoint were recorded. At the last clinical visit, each druse was evaluated based on CFP as to whether it appeared refractile, i.e., containing small bright white dots.[15] Additionally, four FAF stages of drusen were proposed based on previous observations: Stage 1, isoFAF, no obvious FAF alteration but drusen visible on CFP; Stage 2, mildly uniform hyperFAF; Stage 3, a ring of hyperFAF around a center of hypoFAF; and Stage 4, uniformly hypoFAF. With OCT, Stages 3

and 4 demonstrate incomplete RPE and outer retinal atrophy (iRORA) as defined by the Classification of Atrophy Meetings (CAM) group.[18]

Tissue preparation

Sixteen months after the last clinical examination, the patient died of complications of COPD. Globes were recovered 6.25 hours after death by personnel of The Eye-Bank for Sight Restoration (New York USA), opened anteriorly by cornea removal, preserved by immersion in 4% phosphate buffered paraformaldehyde, and shipped overnight on wet ice to Birmingham, Alabama, USA.

The preserved globe with anterior segment removed was imaged with *ex vivo* OCT and NIR (787 nm) prior to histologic processing, as described.[20] An 8×12 mm (vertical x horizontal) full-thickness tissue sample including the fovea and most of the optic nerve head was excised from the eyecup, post-fixed with osmium tannic acid paraphenylenediamine to preserve extracellular lipids, embedded in epoxy resin (PolyBed 812, EMS, Hatfield PA), and oriented for sectioning in a superior to inferior direction. Glass slides with 0.8 μm-thick sections were stained with toluidine blue (left eye, n=90, distance 58 ± 23 μm, range 22 – 134 μm; right eye: n=115, distance 64 ± 9 μm, range 25 – 125 μm). One section per slide was scanned with a 20X objective and a robotic microscope stage (Olympus VSI 120, CellSens; Olympus, Center Valley PA), scaled to tissue units, and centered on the fovea or vertical meridian (where Henle fibers diverge) using a custom plugin for ImageJ (https://imagej.nih.gov/ij/download.html). Selected sections were scanned for detailed review using a 60x oil-immersion objective (numerical aperture =1.42). These were viewed using ImageJ on a monitor at magnifications up to 1240X. For figures, contrast and white balance of images were adjusted to maximize the intensity histogram (Photoshop CS6, Adobe Systems, USA).

Histopathologic review

Ex vivo OCT B-scans (see above) were referenced to the *in vivo* OCT B-scans from the last clinic visit (16 months before death). Histology sections were correlated to *in vivo* B-scans by landmarks for point-by-point OCT-histology correlation. Nineteen sections 240 μm apart were determined to correspond to clinical B-scans for both eyes. These 19 sections served as an anchor that could be combined with information on distance between neighboring sections. All sections from both eyes were evaluated in order to maximize the number of drusen identified and referenced to CFP and FAF.

Drusen visible on both histology section and CFP were included in the analysis. These inclusion criteria in this study allowed the characterization of drusen stages as early as an iso-FAF Stage 1. FAF stage of each druse was determined based on criteria described above. On histology, we measured (ImageJ) drusen height, width of drusen bases, thickness of basal laminar deposit (BLamD) on top of drusen, and the combined height of drusen and BLamD. We also evaluated outer retinal alteration above each druse and components of the druse interior. The outer nuclear layer (ONL) was classified as: normal, thin, dyslaminate,[21] no ONL, and not evaluable. The ELM was classified as: continuous, discontinuous, undetectable, and not evaluable. Photoreceptor inner segments (IS) and outer segments (OS)

were classified as: normal, short OS, no OS-short IS, no IS, and not evaluable. Changes in overlying RPE was classified by the percentage of the druse dome covered: covered (>90%), partly covered (10%−90%), and absent (<10%). Within drusen interiors, we evaluated the presence/ absence of lipid,[22] neovascularization (NV),[19] avascular fibrosis,[23] subducted RPE (individual cells with numerous RPE organelles in the sub-RPE-basal laminar space) [24] and calcified nodules,[16] (recognized by size (>5 μm) and multi-lobed morphology). The abundance of calcified nodules was assessed semi-quantitatively (<25%, 26–50%, 51–75%, and >76% of the cross-sectional area of each druse interior).

Quantitative analysis

Data are presented as percentage of drusen affected with various features. Thicknesses are presented as mean ± standard deviation, calculated with a spreadsheet (Excel Version 16.39, Microsoft).

Results

The evolution of individual drusen on both CFP and FAF during follow-up were reviewed. Figure 2 and 3 show the evolution of soft drusen in an area superior temporal to the fovea in the left and right eyes, respectively, over 9 years of follow-up. Over time, more drusen became visible (Figure 2A–D, 3A–D), and the FAF stages of drusen progressed (Figure 2a–d, 3a–d). These changes can be followed for individual drusen in Figures 2–3 and a group of drusen in Figure 3. In both figures, drusen can be seen to increase in size and become refractile on CFP (Figure 2A1–D1 and A2–D2; Figure 3A1–D1 and 3A2–D2). With one druse in the left eye, the FAF stage progresses from early Stage 3 with very small distinct hypoFAF spots inside the hyperFAF area (Figure 2a1), to Stage 3 with a center of hypoFAF surrounded by a ring of hyperFAF (Figure 2b1), and to Stage 4 with hypoFAF without a ring of hyperFAF (Figure 2c1–d1). Another druse in this eye shows mild hyperFAF (Stage 2) at baseline (Figure 2a2), and then at Stage 3 (Figure 2b2–d2). Figure 3a1–d1 demonstrates that the FAF stage of one druse in the right eye progresses from Stage 2 to early Stage 3, to Stage 3, and then to Stage 4. Figure 3a2–d2 shows a group drusen with isoFAF at baseline (Stage 1) which progress to early Stage 2 with vaguely visible hyperFAF, to Stage 2, and then to early Stage 3.

Drusen visible on both histology and CFP were evaluated and assigned to FAF stages based on clinical FAF appearance. Figure 4 and 5 show the representative clinicopathologic correlation of drusen in four different FAF stages in the left and right eyes, respectively. The retina in the right eye remained better attached than the left eye, allowing a better view of the photoreceptors. CFP and FAF show many drusen in an area superior temporal to the fovea, including four that exemplify FAF Stages 1–4 (Figure 4A,B, 5A,B; teal arrowheads). A druse in Stage 1 is isoFAF, which corresponds on histology to a small soft druse completely covered by an intact RPE layer, long outer segments, and a thick ONL (Figure 4–1, 5–1). Many small calcified nodules are seen in drusen of all subsequent FAF stages. Stage 2 drusen correspond to a soft druse completely covered by the RPE layer (Figure 4–2) in the left eye. In the right eye, a Stage 2 druse is filled with calcified nodules and completely covered by the RPE layer, with very short inner segments lacking outer segments, and a thin

and dyslaminate HFL/ONL (Figure 5–2). A Stage 3 druse corresponds to a druse filled with calcified nodules and partly covered by an RPE layer with a thick BLamD. Above Stage 3 drusen, inner and outer segments are very short (Figure 4–3) or even absent (Figure 5–3), and ONL is thin. A Stage 4 druse corresponds to a druse filled with calcified nodules and covered by persistent BLamD lacking RPE (Figure 4–4, 5–4).

We analyzed the histologic characteristics of 166 drusen that were also visible in CFP, assigned to 1 of the 4 FAF stages. Among these 166, 26 were Stage 1, 65 were Stage 2, 63 were Stage 3, and 12 were Stage 4. Table 1 shows druse height and width and BLamD thickness, stratified by FAF stages. The height of drusen in Stages 1–4 were 25.1 ± 7.2 μm, 43.9 ± 17.8 μm, 66.7 ± 34.0 μm, and 68.5 ± 24.8 μm, respectively. The width of drusen in Stages 1–4 were 77.0 ± 33.3 μm, 131.7 ± 61.0 μm, 176.8 ± 90.4 μm, and 208.1 ± 80.6 μm, respectively. The thickness of BLamD in Stages 1–4 were 4.6 ± 3.7 μm, 7.5 ± 5.4 μm, 12.6 ± 7.0 μm, and 6.7 ± 2.7 μm, respectively. The total height of drusen plus BLamD in Stages 1–4 were 29.7 ± 9.5 μm, 51.4 ± 20.0 μm, 79.4 ± 37.4 μm, and 75.2 ± 26.3 μm, respectively.

Figure 6 shows outer retinal alterations, as determined by histologic analysis, associated with 166 drusen at different FAF stages. Figure 6A–D shows ONL, ELM, IS and OS, and RPE, respectively, in 4 separate bar graphs. Stage 1 drusen tend to have a normal ONL (96% of 166 drusen), continuous ELM (96%), normal IS and OS (65%) and complete coverage by RPE (96%). Stage 2 drusen tend to have a normal ONL (68%), continuous ELM (85%), short OS (66%), and complete coverage by RPE (98%). Stage 3 drusen tend to have a thin ONL (57%), continuous ELM (81%), no OS and short IS (43%) or no IS (32%), and partial coverage by RPE (67%). Stage 4 drusen tend to lack detectable ONL (67%), ELM (67%), IS or OS (75%), and RPE (100%).

Figure 7 shows drusen components by histology and drusen refractility on CFP, a measure of druse calcification, at different FAF stages. Figure 7A shows druse components, including lipid, NV, avascular fibrosis, subducted RPE and calcified nodules. Figure 7B shows the proportion of drusen cross-sections occupied by calcified nodules. Figure 7C shows the degree of refractility. We found that the percentage of drusen with lipid material decreased with increasing FAF stages, and the percentage of drusen with other components, especially calcified nodules, increased with increasing FAF stages (Figure 7A). Within individual drusen, those at FAF Stage 1 and 2 tend to have a smaller mass of calcified nodules (< 25% of the cross-sectional area), while drusen in Stage 3 and Stage 4 tend to have a larger mass of nodules (> 75% of the cross-sectional area) (Figure 7B). Drusen in FAF Stage 4 (82 %) tend to be more refractile on CFP than drusen in FAF Stage 3 (24 %), Stage 2 (6 %) and Stage 1 (0 %) (Figure 7C).

Discussion

A sequence of events preceding atrophy, visible in FAF, was hinted at in our prior publications.[15, 16] Here we refined and quantified this sequence via direct clinicopathologic correlation of drusen-associated atrophy in two eyes of one patient with advanced AMD monitored on multimodal imaging spanning an extended follow-up. Our data indicate that both photoreceptors and RPE contribute to characteristic FAF patterns atop drusen.

By revealing retinal layers and stages involved in drusen-associated atrophy, our findings provide a new level of anatomic ground truth for interpreting FAF imaging in AMD. Our data support a staging system proposed by the Classification of Atrophy Meeting group for drusen-associated atrophy,[18] extending it backward in time to early disease. Thus, our data can spur the development of new imaging biomarkers.

Our studies were informed by a previously established partial timeline of drusen-associated atrophy. Suzuki et al reported refractile drusen as a stage of regression marked by a progression from rings of hyperFAF to uniform hypoFAF.[15] Tan et al demonstrated that calcified nodules in drusen indicated an increased progression risk. These authors concluded from loss of FAF over drusen with nodules that the RPE was in an agonal state.[16] We previously showed by histology of the current case[18] ELM descents delimiting areas of total photoreceptor and RPE depletion in two atrophic spots initiated at the sites of drusen. We also showed evidence of Müller glia entering each druse from above, consistent with evidence that Müller glia[25] can anchor atrophic retina to Bruch's membrane.[23] This prior work, while valuable, did not inform about FAF variation at stages preceding frank atrophy. By histologic analysis of 166 drusen at four stages defined in this report, we demonstrated discontinuous ELM at Stage 3 and undetectable ELM at Stage 4 atop individual drusen, thus verifying this hypothesized progression sequence of atrophy. Initially, this atrophy is too small to qualify as cRORA, making it iRORA.[18] Previously, we demonstrated how one druse could initiate cRORA.[26]

Our use of registered multimodal imaging and a comprehensive accounting allowed a view of very early changes. We infer that all drusen assessed in this study started as soft because Stage 1 has high lipid content and lipid is present in declining quantities in Stages 2–4. Drusen at FAF Stage 1 were by definition visible in CFP and not in FAF. It is possible that color change, especially after brightness and contrast adjustment, is more readily detected than intensity differences in FAF. Further, our data show that uniform hyperFAF atop drusen (FAF Stage 2) occurred earlier than any stage with RPE atrophy. While 4% of Stage 1 and 2% of Stage 2 drusen showed only partial coverage by RPE, this was likely due to progression during the 16 months between the last clinic visit and patient death. HyperFAF on top of drusen has been attributed by previous authors to high intracellular accumulation of L/ML, L/ML redistribution within individual RPE cells,[6] and hyperreflective foci within the retina above drusen.[27] In rhesus macaques, hyperFAF was directly correlated to RPE hypertrophy overlying drusen,[28] in contrast to RPE atrophy overlying drusen in humans.

Previous studies indicated the potential of photoreceptor participation in modulating FAF signal. Bleaching photopigment in advance of an FAF imaging session yields hyperFAF.[10] In disorders of outer retina that damage photoreceptors, FAF cannot be increased by bleaching.[12] Other authors showed that variation in clinical FAF strongly correlates with drusen size and disruption of the IS-OS band (EZ).[29] Herein, by histology we observed that photoreceptors were short above all drusen in FAF Stage 2, which also had complete coverage by RPE and continuous ELM. Our data support the idea that photoreceptor shortening underlies uniform hyperFAF above drusen, as the earliest visible FAF sign of drusen-associated atrophy. These screening effects are independent of the fact that molecular

precursors of RPE fluorophores originate in the photoreceptors and are internalized daily by RPE during outer segment disk shedding.[30]

FAF Stage 3, comprised of a hyperFAF ring around a hypoFAF center, is transitional between uniform hyperFAF and uniform hypoFAF. HyperFAF rings were first attributed to individual drusen by Delori et al.[14] Without OCT, this pattern was thought to represent displacement of overlying RPE and/or L/ML content without actual loss of RPE. For example, RPE could redistribute over a druse dome[6] such that cells are thin on top and thick around the bottom. However, our findings indicate that RPE atrophy with limited redistribution together with photoreceptor shortening can account for hyperFAF rings. As discussed, photoreceptor shortening contributed to uniform hyperFAF in Stage 2, a newly defined, logical precursor to Stage 3. In Stage 3, RPE atrophy starting at the druse apex forms a hypoFAF center inside the hyperFAF area that progressively assumes a ring shape. Indeed, a gap in the RPE layer is visible in histology of Stage 3 drusen (Figure 4–3, 5–3); thick RPE does not border the gap. HyperFAF rings were also previously seen around cuticular drusen,[17] which are overall smaller than soft drusen. Interestingly rings of hyperpigmentation correspond to RPE thickening at the base of peripheral hard drusen.[31] Widefield imaging makes it possible to check whether these rings are also hyperFAF

Our histologic analysis of drusen visible in CFP clarifies the imaging features of calcified drusen. By ophthalmoscopy, refractile or glistening deposits regularly appear in areas where drusen regress, before the onset of cRORA.[32] By OCT, drusen can develop hyporeflective interiors, sometimes with overlying punctate reflective dots. In longitudinal observation studies, these findings confer risk for progression to end-stages.[16, 33] Direct clinicopathologic correlation and nano-analytic techniques established that hyporeflective interiors correspond to multi-lobular nodules of hydroxyapatite 20–100 μm in diameter.[16] These contrast with smaller magnesium containing hydroxyapatite spherules (0.5–20 μm diameter) appearing in nearly all drusen.[16] These smaller features were initially proposed (by Suzuki et al including author CAC) as sources of punctate reflectivity.[15] Our current data indicate that histologic drusen with nodules correlate to clinical drusen with hyporeflective cores, punctate reflectivity, and reflective dots. The prior attribution of hyperreflectivity to spherules alone should be revised. In the current case, the high percentage of drusen with calcific nodules (94% and 100% in Stages 3 and 4, respectively) supports the idea that nodules signify dying RPE.

We herein highlight essential roles for OCT, magnification, and individual lesion phenotyping as tools for interpreting FAF. Our histologic data complement studies of clinical OCT features associated with FAF variation, including drusen size, hyperreflective foci, disruption of EZ, outer nuclear layer thinning, and choroidal hypertransmission.[27, 29, 34] Recent authors concluded that FAF changes appeared earlier than subsidence of outer plexiform layer and appearance of hyporeflective wedges in HFL (i.e., nascent geographic atrophy)[35]; we examined retinal layers closer to the drusen and thus affected even earlier in AMD progression. We emphasize magnification, because abundant information can be gleaned simply by viewing FAF images that are enlarged (Figures 2 and 3). Retinal neurons are 1/10 the size of brain neurons, and photoreceptors and RPE are very small, befitting their joint role as a sensory sampling array. Finally, although

quantitative FAF, an aggregate per-eye metric, has not yet revealed trends among eyes with drusen,[36] new tools now allow point-by-point comparison of individual lesions to a normative database.[37]

Our data reinforce the clinical utility of FAF for AMD and motivate further laboratory study of FAF signal sources in appropriate systems. A new narrative on RPE L/ML is emerging from precise human eye pathology linked to clinical imaging. Long-standing concepts on RPE L/ML are that it is phototoxic and contributory to both RPE cell death and drusen biogenesis.[38] These ideas contribute to the rationale for visual cycle modulators as AMD therapies, which have not met clinical trial endpoints so far.[39] These conclusions were based on molecular assay techniques with limited or no spatial resolution (e.g., whole eye cup extraction), non-physiologic experiments using low-fidelity cell systems, and animal models lacking all-cone foveas and steep gradients in photoreceptor density.[40, 41] In contrast, enumeration of photoreceptors and RPE using flat-mounts that preserve foveal position for accuracy have failed to link L/ML accumulation to loss of photoreceptors or RPE with aging and instead show early L/ML redistribution and loss in AMD.[5, 7, 42] Assay techniques that preserve retinal topography have shown that one compound thought to be cytotoxic (A2E) is detectable at lower levels in macula than periphery.[43] Highly differentiated and polarized RPE cells in culture clear A2E efficiently.[44] From these and other data, RPE L/ML may be viewed as benign; a role in retinoid balance is possible.

Strengths of this study include the direct clinicopathologic correlation of eyes that were imaged serially with FAF during life, short death-to-preservation interval that ensured attachment of neurosensory retina to RPE, high-resolution histology, and point-to-point alignment of a large sample of individual drusen in FAF, CFP, and histology. Limitations include the lack of FAF imaging with the commonly used 488 nm wavelength, and lack of autofluorescence quantification for individual cells and organelles. Our data are relevant to drusen fates seen in this one case and may not be generalizable to other drusen fates (e.g., coalescence into pigment epithelial detachments, atrophy without nodules, or resolution without atrophy). Nevertheless, this report represents the first direct clinicopathologic correlations of FAF variation in AMD. Data support photoreceptor participation in an intermediate stage of hyperFAF before atrophy and the loss of ELM atop every atrophic druse examined. Atrophy proceeds one druse at a time. Such findings could lead to insights about new therapeutic approaches and identification of new clinical study endpoints.

Acknowledgments

We thank Brian McArdle of The Eye-Bank for Sight Restoration (NYC) for timely retrieval of donor eyes.

Financial support:

This work was supported by Genentech/ Hoffman LaRoche, Heidelberg Engineering, The Macula Foundation, Inc., New York, NY; unrestricted funds to the Department of Ophthalmology and Visual Sciences (UAB) from Research to Prevent Blindness, Inc., and EyeSight Foundation of Alabama. Basic research in autofluorescence imaging was funded by NIH R01EY06109 and R01EY027948 (CAC)

References

1. Yung M, Klufas MA, Sarraf D. Clinical applications of fundus autofluorescence in retinal disease. Int J Retina Vitreous. 2016;2:12. [PubMed: 27847630]
2. Wing GL, Blanchard GC, Weiter JJ. The topography and age relationship of lipofuscin concentration in the retinal pigment epithelium. Invest Ophthalmol Vis Sci. 1978;17(7):601–7. [PubMed: 669891]
3. Feeney L. Lipofuscin and melanin of human retinal pigment epithelium. Fluorescence, enzyme cytochemical, and ultrastructural studies. Invest Ophthalmol Vis Sci. 1978;17(7):583–600. [PubMed: 669890]
4. Rudolf M, Vogt SD, Curcio CA, et al. Histologic basis of variations in retinal pigment epithelium autofluorescence in eyes with geographic atrophy. Ophthalmology. 2013;120(4):821–8. [PubMed: 23357621]
5. Ach T, Huisingh C, McGwin G Jr., et al. Quantitative autofluorescence and cell density maps of the human retinal pigment epithelium. Invest Ophthalmol Vis Sci. 2014;55(8):4832–41. [PubMed: 25034602]
6. Ach T, Tolstik E, Messinger JD, Zarubina AV, Heintzmann R, Curcio CA. Lipofuscin redistribution and loss accompanied by cytoskeletal stress in retinal pigment epithelium of eyes with age-related macular degeneration. Invest Ophthalmol Vis Sci. 2015;56(5):3242–52. [PubMed: 25758814]
7. Gambril JA, Sloan KR, Swain TA, et al. Quantifying retinal pigment epithelium dysmorphia and loss of histologic autofluorescence in age-related macular degeneration. Invest Ophthalmol Vis Sci. 2019;60(7):2481–93. [PubMed: 31173079]
8. Bermond K, Wobbe C, Tarau IS, et al. Autofluorescent granules of the human retinal pigment epithelium: phenotypes, intracellular distribution, and age-related topography. Invest Ophthalmol Vis Sci. 2020;61(5):35.
9. Sears AE, Bernstein PS, Cideciyan AV, et al. Towards treatment of stargardt disease: workshop organized and sponsored by the foundation fighting blindness. Transl Vis Sci Technol. 2017;6(5):6.
10. Theelen T, Berendschot TT, Boon CJ, Hoyng CB, Klevering BJ. Analysis of visual pigment by fundus autofluorescence. Exp Eye Res. 2008;86(2):296–304. [PubMed: 18096158]
11. Delori F, Greenberg JP, Woods RL, et al. Quantitative measurements of autofluorescence with the scanning laser ophthalmoscope. Invest Ophthalmol Vis Sci. 2011;52(13):9379–90. [PubMed: 22016060]
12. Freund KB, Mrejen S, Jung J, Yannuzzi LA, Boon CJ. Increased fundus autofluorescence related to outer retinal disruption. JAMA Ophthalmol. 2013;131(12):1645–9. [PubMed: 24136134]
13. Wang JJ, Rochtchina E, Lee AJ, et al. Ten-year incidence and progression of age-related maculopathy: the blue mountains eye study. Ophthalmology. 2007;114(1):92–8. [PubMed: 17198852]
14. Delori FC, Fleckner MR, Goger DG, Weiter JJ, Dorey CK. Autofluorescence distribution associated with drusen in age-related macular degeneration. Invest Ophthalmol Vis Sci. 2000;41(2):496–504. [PubMed: 10670481]
15. Suzuki M, Curcio CA, Mullins RF, Spaide RF. Refractile drusen: clinical imaging and candidate histology. Retina. 2015;35(5):859–65. [PubMed: 25768253]
16. Tan ACS, Pilgrim MG, Fearn S, et al. Calcified nodules in retinal drusen are associated with disease progression in age-related macular degeneration. Sci Transl Med. 2018;10(466).
17. Balaratnasingam C, Cherepanoff S, Dolz-Marco R, et al. Cuticular drusen: clinical phenotypes and natural history defined using multimodal imaging. Ophthalmology. 2018;125(1):100–18. [PubMed: 28964580]
18. Guymer RH, Rosenfeld PJ, Curcio CA, et al. Incomplete retinal pigment epithelial and outer retinal atrophy in age-related macular degeneration: classification of atrophy meeting report 4. Ophthalmology. 2020;127(3):394–409. [PubMed: 31708275]
19. Chen L, Messinger JD, Sloan KR, et al. Nonexudative macular neovascularization supporting outer retina in age-related macular degeneration: a clinicopathologic correlation. Ophthalmology. 2020;127(7):931–47. [PubMed: 32247535]

20. Curcio CA, Balaratnasingam C, Messinger JD, Yannuzzi LA, Freund KB. Correlation of type 1 neovascularization associated with acquired vitelliform lesion in the setting of age-related macular degeneration. Am J Ophthalmol. 2015;160(5):1024–33 e3. [PubMed: 26255578]
21. Li M, Huisingh C, Messinger J, et al. Histology of geographic atrophy secondary to age-related macular degeneration: a multilayer approach. Retina. 2018;38(10):1937–53. [PubMed: 29746415]
22. Chen L, Messinger JD, Sloan KR, et al. Abundance and multimodal visibility of soft drusen in early age-related macular degeneration: a clinicopathologic correlation. Retina. 2020;40(8):1644–8. [PubMed: 32568988]
23. Li M, Dolz-Marco R, Huisingh C, et al. Clinicopathologic correlation of geographic atrophy secondary to age-related macular degeneration. Retina. 2019;39(4):802–16. [PubMed: 30839495]
24. Zanzottera EC, Messinger JD, Ach T, Smith RT, Curcio CA. Subducted and melanotic cells in advanced age-related macular degeneration are derived from retinal pigment epithelium. Invest Ophthalmol Vis Sci. 2015;56(5):3269–78. [PubMed: 26024109]
25. Edwards MM, McLeod DS, Bhutto IA, Villalonga MB, Seddon JM, Lutty GA. Idiopathic preretinal glia in aging and age-related macular degeneration. Exp Eye Res. 2016;150:44–61. [PubMed: 26220834]
26. Chen L, Li M, Messinger JD, Ferrara D, Curcio CA, Freund KB. Recognizing atrophy and mixed-type neovascularization in age-related macular degeneration via clinicopathologic correlation. Transl Vis Sci Technol. 2020;9(8):8.
27. Gobel AP, Fleckenstein M, Heeren TF, Holz FG, Schmitz-Valckenberg S. In-vivo mapping of drusen by fundus autofluorescence and spectral-domain optical coherence tomography imaging. Graefes Arch Clin Exp Ophthalmol. 2016;254(1):59–67. [PubMed: 25904296]
28. Tran TM, Kim S, Lin KH, et al. Quantitative fundus autofluorescence in rhesus macaques in aging and age-related drusen. Invest Ophthalmol Vis Sci. 2020;61(8):16.
29. Landa G, Rosen RB, Pilavas J, Garcia PM. Drusen characteristics revealed by spectral-domain optical coherence tomography and their corresponding fundus autofluorescence appearance in dry age-related macular degeneration. Ophthalmic Res. 2012;47(2):81–6. [PubMed: 21757965]
30. Sparrow JR, Wu Y, Nagasaki T, Yoon KD, Yamamoto K, Zhou J. Fundus autofluorescence and the bisretinoids of retina. Photochem Photobiol Sci. 2010;9(11):1480–9. [PubMed: 20862444]
31. Lewis H, Straatsma BR, Foos RY, Lightfoot DO. Reticular degeneration of the pigment epithelium. Ophthalmology. 1985;92(11):1485–95. [PubMed: 4080322]
32. Klein ML, Ferris FL 3rd, Armstrong J, et al. Retinal precursors and the development of geographic atrophy in age-related macular degeneration. Ophthalmology. 2008;115(6):1026–31. [PubMed: 17981333]
33. Ouyang Y, Heussen FM, Hariri A, Keane PA, Sadda SR. Optical coherence tomography-based observation of the natural history of drusenoid lesion in eyes with dry age-related macular degeneration. Ophthalmology. 2013;120(12):2656–65. [PubMed: 23830761]
34. Flores R, Carneiro A, Serra J, et al. Correlation study between drusen morphology and fundus autofluorescence. Retina. 2020.
35. Rodríguez A, Biarnés M, Coco-Martin RM, Sala-Puigdollers A, Monés J. Early detection of incipient retinal pigment epithelium atrophy overlying drusen with fundus autofluorescence vs. spectral domain optical coherence tomography. Journal of Ophthalmology. 2020;2020:1–8.
36. Reiter GS, Told R, Schlanitz FG, et al. Impact of drusen volume on quantitative fundus autofluorescence in early and intermediate age-related macular degeneration. Invest Ophthalmol Vis Sci. 2019;60(6):1937–42. [PubMed: 31050721]
37. Kleefeldt N, Bermond K, Tarau IS, et al. Quantitative fundus autofluorescence: advanced analysis tools. Transl Vis Sci Technol. 2020;9(8):2.
38. Yoon KD, Yamamoto K, Ueda K, Zhou J, Sparrow JR. A novel source of methylglyoxal and glyoxal in retina: implications for age-related macular degeneration. PLoS One. 2012;7(7):e41309. [PubMed: 22829938]
39. Rosenfeld PJ, Dugel PU, Holz FG, et al. Emixustat hydrochloride for geographic atrophy secondary to age-related macular degeneration: a randomized clinical trial. Ophthalmology. 2018;125(10):1556–67. [PubMed: 29716784]

40. Eldred GE, Lasky MR. Retinal age pigments generated by self-assembling lysosomotropic detergents. Nature. 1993;361(6414):724–6. [PubMed: 8441466]

41. Mata NL, Weng J, Travis GH. Biosynthesis of a major lipofuscin fluorophore in mice and humans with ABCR-mediated retinal and macular degeneration. Proc Natl Acad Sci U S A. 2000;97(13):7154–9. [PubMed: 10852960]

42. Curcio CA, Millican CL, Allen KA, Kalina RE. Aging of the human photoreceptor mosaic: evidence for selective vulnerability of rods in central retina. Invest Ophthalmol Vis Sci. 1993;34(12):3278–96. [PubMed: 8225863]

43. Ablonczy Z, Higbee D, Anderson DM, et al. Lack of correlation between the spatial distribution of A2E and lipofuscin fluorescence in the human retinal pigment epithelium. Invest Ophthalmol Vis Sci. 2013;54(8):5535–42. [PubMed: 23847313]

44. Zhang Q, Presswalla F, Calton M, et al. Highly differentiated human fetal rpe cultures are resistant to the accumulation and toxicity of lipofuscin-like material. Invest Ophthalmol Vis Sci. 2019;60(10):3468–79. [PubMed: 31408109]

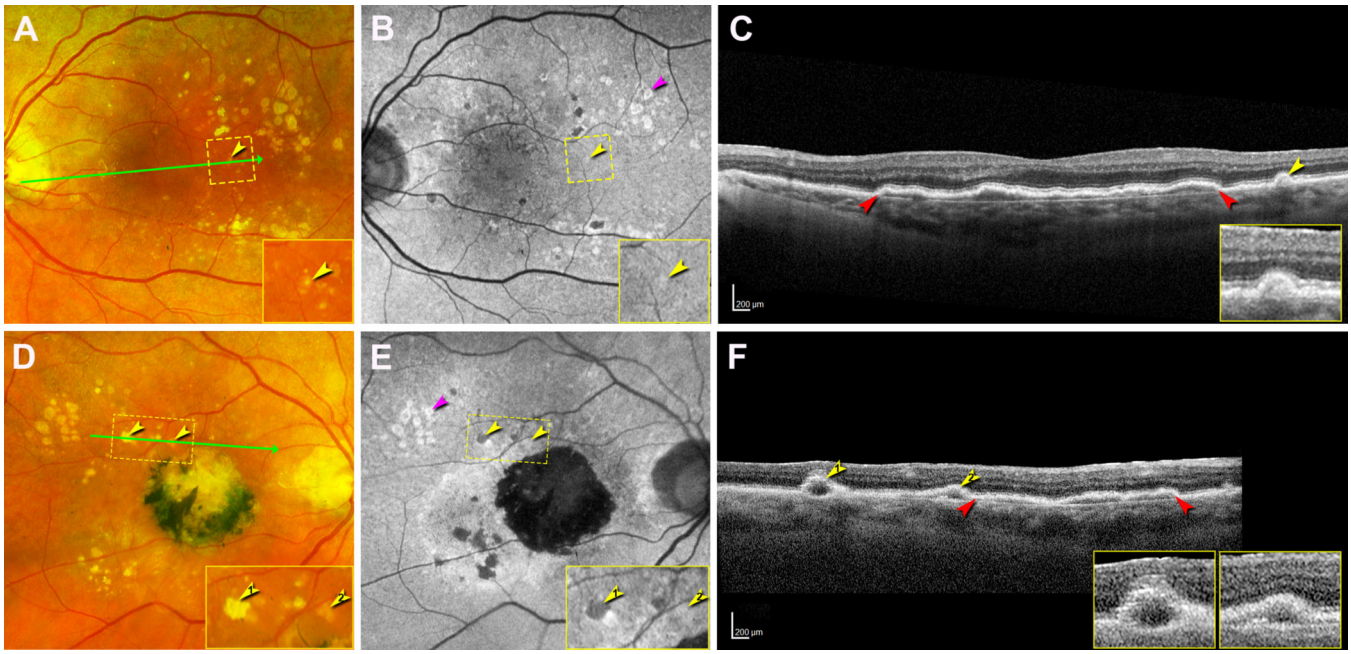

Figure 1. Multimodal imaging showing drusen at the last clinical visit.

All images were acquired 16 months before patient death. A, B, D, E were acquired with the Optos California. **A-C.** Left eye. **A.** Color fundus photograph (CFP) shows soft and refractile drusen that mostly spare the central macula. A small druse (yellow arrowhead) inside the yellow dashed frame is magnified in the inset. The green arrow indicates the location and direction of the corresponding optical coherence tomography (OCT) B-scan in panel C. **B.** With fundus autofluorescence (FAF) the small druse shows mild hyperFAF (yellow arrowhead, inset). A group of drusen have rings of hyperFAF around centers of hypoFAF (pink arrowhead). **C.** OCT B-scan shows an extensive shallow irregular retinal pigment epithelium (RPE) elevation (SIRE, red arrowheads), a small druse covered by RPE and overlying external limiting membrane (ELM) (inset). **D-F.** Right eye. **D.** CFP shows a central subretinal fibrosis with black pigment, and both refractile and soft drusen (yellow arrowheads, magnified in inset), mostly superior temporal to the fovea. The green arrow indicates the location of corresponding OCT B-scan in panel F. **E.** FAF shows the refractile druse to demonstrate hypoFAF and the soft drusen to show mild hyperFAF (yellow arrowheads, inset). A druse group has rings of hyperFAF around centers of hypoFAF (pink arrowhead). **F.** OCT B-scan shows two drusen (yellow arrowheads) on the left and SIRE (red arrowheads) on the right. Each druse has a hyporeflective core. The right druse is covered by RPE and ELM (insets). These bands are not visible over the left druse.

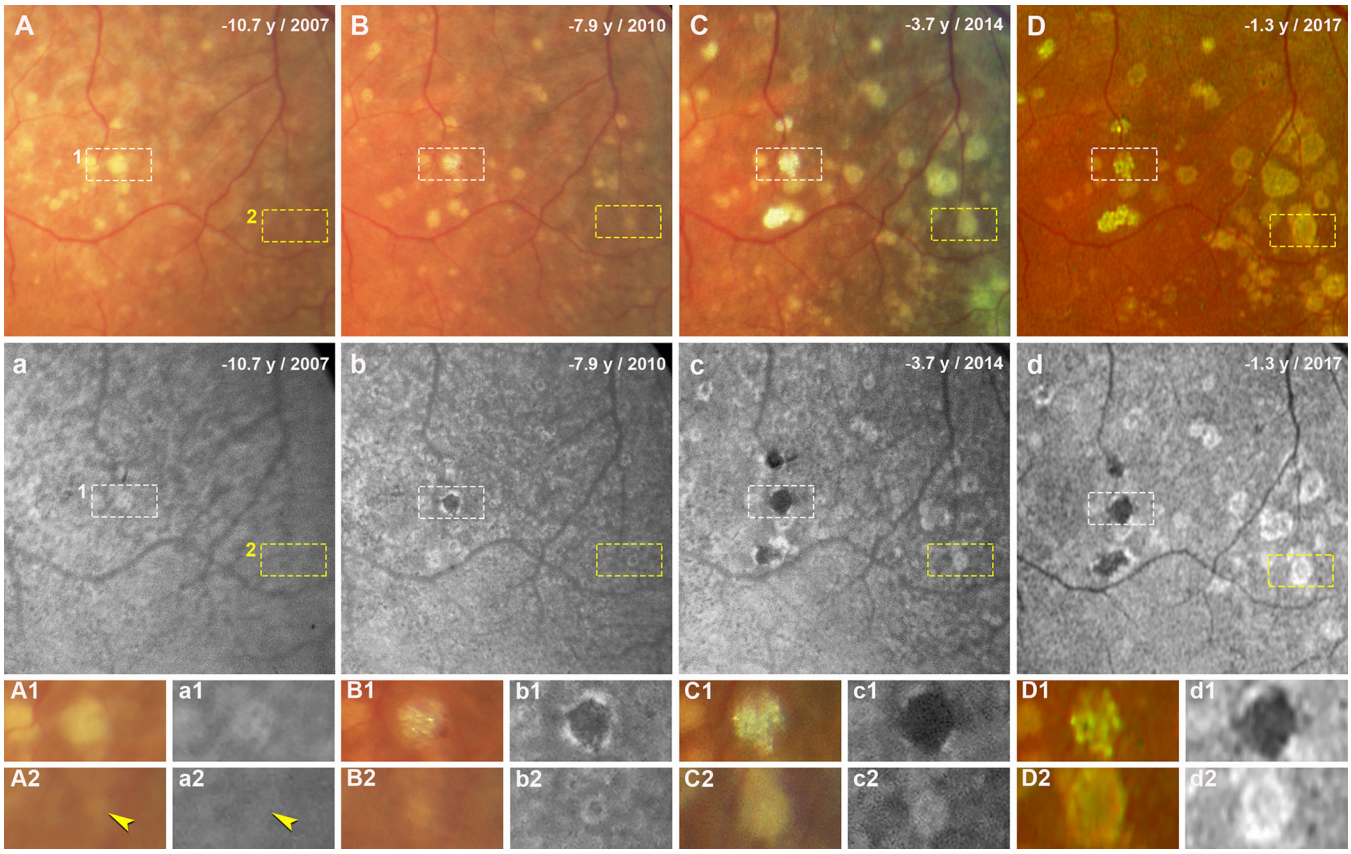

Figure 2. Evolution of soft drusen in the left eye over 9 years of follow-up.

Images in A-D and a-d were taken at four time points, indicated as years before patient death. A-C and a-c were acquired with the Topcon TRC-50IX fundus camera; D and d were acquired with the Optos California. **A-D.** Color fundus photographs (CFP) show soft drusen superior temporal to the fovea. White (1) and yellow (2) dashed frames show two drusen that are magnified in panels A1-D1 and A2-D2, respectively. **a-d.** Fundus autofluorescence (FAF) in the same area shows the same drusen. Drusen in white (1) and yellow (2) dashed frames are magnified in panels a1-d1 and a2-d2, respectively. **A1, a1.** Druse 1 at baseline (10.7 years before death) has very small distinct hypoFAF spots inside the hyperFAF area. **B1, b1.** 7.9 years before death, this druse has become refractile on CFP, and appears on FAF as expanded hypoFAF surrounded by a hyperFAF edge. **C1, c1.** 3.7 years before death, the druse is glistening on CFP and hypoFAF on FAF. **D1, d1.** 1.3 years before death, the glistening druse still shows hypoFAF. **A2, a2.** Druse 2 at baseline having a soft edge on CFP and a mildly hyperFAF on FAF (yellow arrowheads). **B2, b2.** Druse has expanded and appearing on FAF as a ring of hyperFAF around a center of hypoFAF. **C2, c2.** Druse has expanded further and appearing on FAF as hypoFAF spots inside hyperFAF. **D2, d2.** Druse with defined edge on CFP showing on FAF as a ring of hyperFAF around a center of hypoFAF.

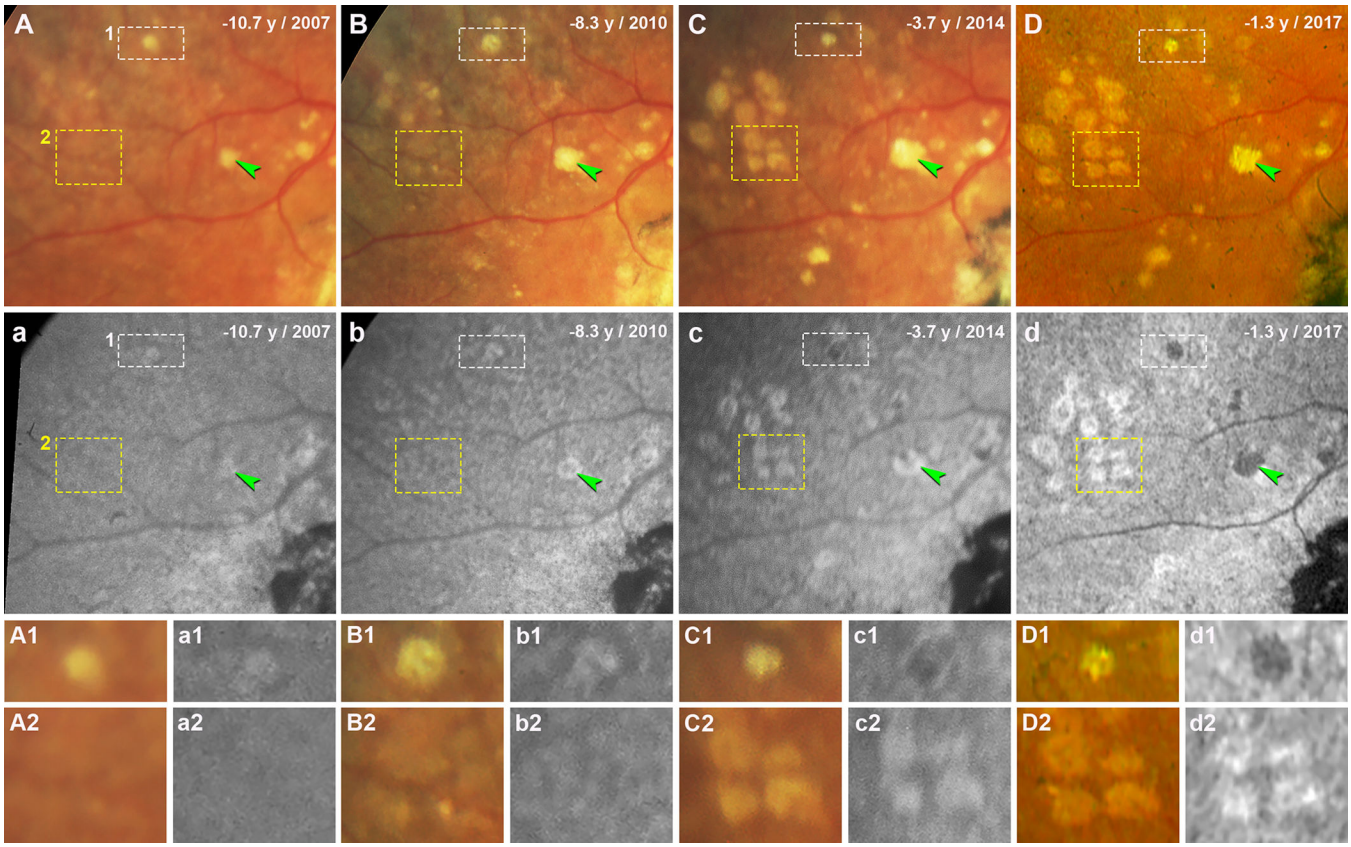

Figure 3. Evolution of soft drusen in the right eye over 9 years of follow-up.

Images in A-D and a-d were taken at four time points, indicated as years before patient death. A-C and a-c were acquired with the Topcon TRC-50IX fundus camera; D and d were acquired with the Optos California. **A-D.** Color fundus photographs (CFP) show soft drusen superior temporal to the fovea. Green arrowheads indicate a druse expanding over time (A-C) and becoming refractile (D). White (1) and yellow (2) dashed frames show drusen that are magnified in panels A1-D1 and A2-D2, respectively. **a-d.** Fundus autofluorescence (FAF) in the same area shows the same drusen. Green arrowheads indicate the same druse as in A-D, appearing as mildly hyperFAF (a), a ring of hyperFAF around a center of hypoFAF (b, c), and uniformly hypoFAF (d). Drusen in white (1) and yellow (2) dashed frames are magnified in panels a1-d1 and a2-d2, respectively. **A1, a1.** Druse 1 at baseline (10.7 years before death) appears mildly hyperFAF. **B1, b1.** 8.3 years before death, this druse has expanded and developed a more defined edge, appearing on FAF as a hypoFAF spot inside the hyperFAF. **C1, c1.** 3.7 years before death, the druse overall shrank and became refractile, and the hypoFAF spot expanded. **D1, d1.** 1.3 years before death, the druse is still refractile and is hypoFAF. **A2, a2.** Drusen group 2 at baseline can be barely observed on CFP, appearing on FAF as isoAF. **B2, b2.** Drusen are expanding in CFP and exhibit a variable FAF signal. **C2, c2.** Four drusen having a uniform hyperFAF. **D2, d2.** Four drusen with more defined edges on CFP showing hypoFAF spots inside the hyperFAF.

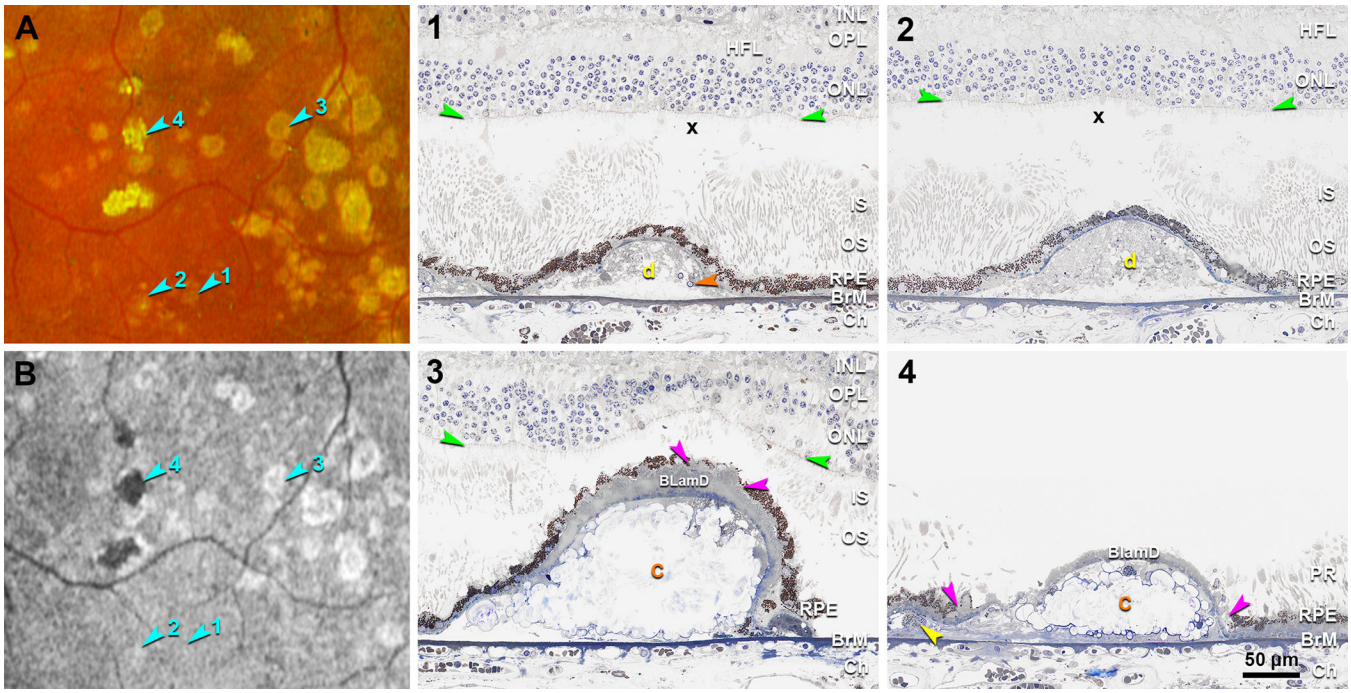

Figure 4. Clinicopathologic correlation of drusen FAF stages in the left eye.

A, B. Color fundus photograph (CFP) and fundus autofluorescence (FAF) (Optos California) in an area superior temporal to the fovea in the left eye, acquired 16 months before patient death. Teal arrowheads indicate four drusen at FAF Stages 1–4. **1–4.** Histology of four drusen shown in panel A and B. (**1**) Druse in Stage 1 is isoFAF (teal arrowhead 1 in B), corresponds on histology to a small druse covered by a continuous RPE layer, long outer segments, and a thick ONL. Orange arrowhead, calcified nodule. X, post-mortem bacillary layer detachment. (**2**) Druse in Stage 2 is hyperFAF (teal arrowhead 2 in B), corresponds on histology to a soft druse covered by a continuous RPE layer. Retina was artifactually detached and digitally approximated to the RPE. Outer segments attached to RPE adjacent to the druse are long. The section doesn't cross the refractile spot inside this druse shown on CPF. (**3**) Druse in Stage 3 shows a ring of hyperFAF around a center of hypoFAF (teal arrowhead 3 in B) and on histology corresponds to a fully calcified druse covered by a very thick layer of BLamD and discontinuous RPE. Pink arrowheads indicate a small gap on RPE. Above this gap, inner and outer segments are very short, and the ONL is thinned. Artifactual retinal detachment was digitally approximated to the RPE. (**4**) Druse in Stage 4 is hypoFAF (teal arrowhead 4 in B) and on histology corresponds to a fully calcified druse covered by persistent BLamD without RPE. In this artefactually detached retina, photoreceptor outer segments contact RPE adjacent to the druse. Pink arrowheads indicate the free edge of RPE; yellow arrowhead indicates a subducted RPE cell. Orange c, calcified druse; Yellow d, druse; INL, inner nuclear layer; OPL, outer plexiform layer; HFL, Henle fiber layer; ONL, outer nuclear layer; ELM, external limiting membrane (green arrowheads); PR, photoreceptors; IS, inner segment; OS, outer segment; RPE, retinal pigment epithelium; BLamD, basal laminar deposit; BrM, Bruch's membrane; Ch, choroid.

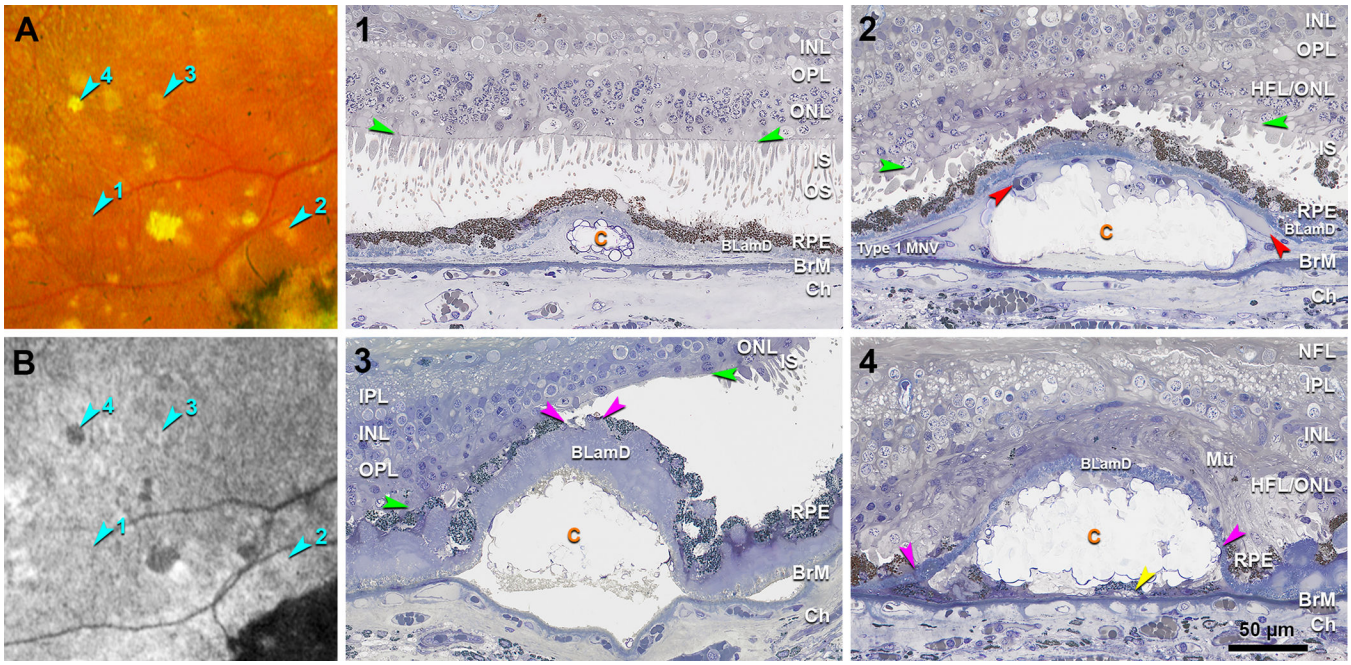

Figure 5. Clinicopathologic correlation of drusen FAF stages in the right eye.

A, B. Color fundus photograph (CFP) and fundus autofluorescence (FAF) (Optos California) in an area superior temporal to the fovea in the right eye, acquired 16 months before patient death. Teal arrowheads indicate four drusen at FAF Stages 1–4. **1–4.** Histology of four drusen shown in panel A and B. (**1**) Druse in Stage 1 is isoFAF (teal arrowhead 1 in B) and corresponds on histology to a small druse with calcific nodules, covered by a continuous RPE layer, almost intact photoreceptors, and a thick ONL. (**2**) Druse in Stage 2 is hyperFAF (teal arrowhead 2 in B) and corresponds on histology to a calcified druse covered by a continuous RPE layer, very short inner segments lacking outer segments, and a thin and dyslaminate ONL-HFL. Red arrowheads indicate vessel lumens of type 1 MNV. (**3**) Druse in Stage 3 appears as a ring of hyperFAF around a center of hypoFAF (teal arrowhead 3 in B) and corresponds on histology to a calcified druse covered by very thick BLamD and discontinuous RPE layer. Pink arrowheads indicate a small gap on RPE. Inner and outer segments are absent above the druse and present but short next to the druse. (**4**) Druse in Stage 4 is hypoFAF (teal arrowhead 4 in B) and corresponds on histology to a calcified druse covered by thin persistent BLamD without RPE and photoreceptors. Pink arrowheads indicate the free edge of RPE, retracting from an initiating atrophic spot; yellow arrowhead indicates a subducted RPE cell. Mü, Müller glia; Orange c, calcified druse; MNV, macular neovascularization; NFL, nerve fiber layer; IPL, inner plexiform layer; INL, inner nuclear layer; OPL, outer plexiform layer; HFL, Henle fiber layer; ONL, outer nuclear layer; HFL/ONL, dyslamination of HFL and ONL; ELM, external limiting membrane (green arrowheads); IS, inner segment; OS, outer segment; RPE, retinal pigment epithelium; BLamD, basal laminar deposit; BrM, Bruch’s membrane; Ch, choroid.

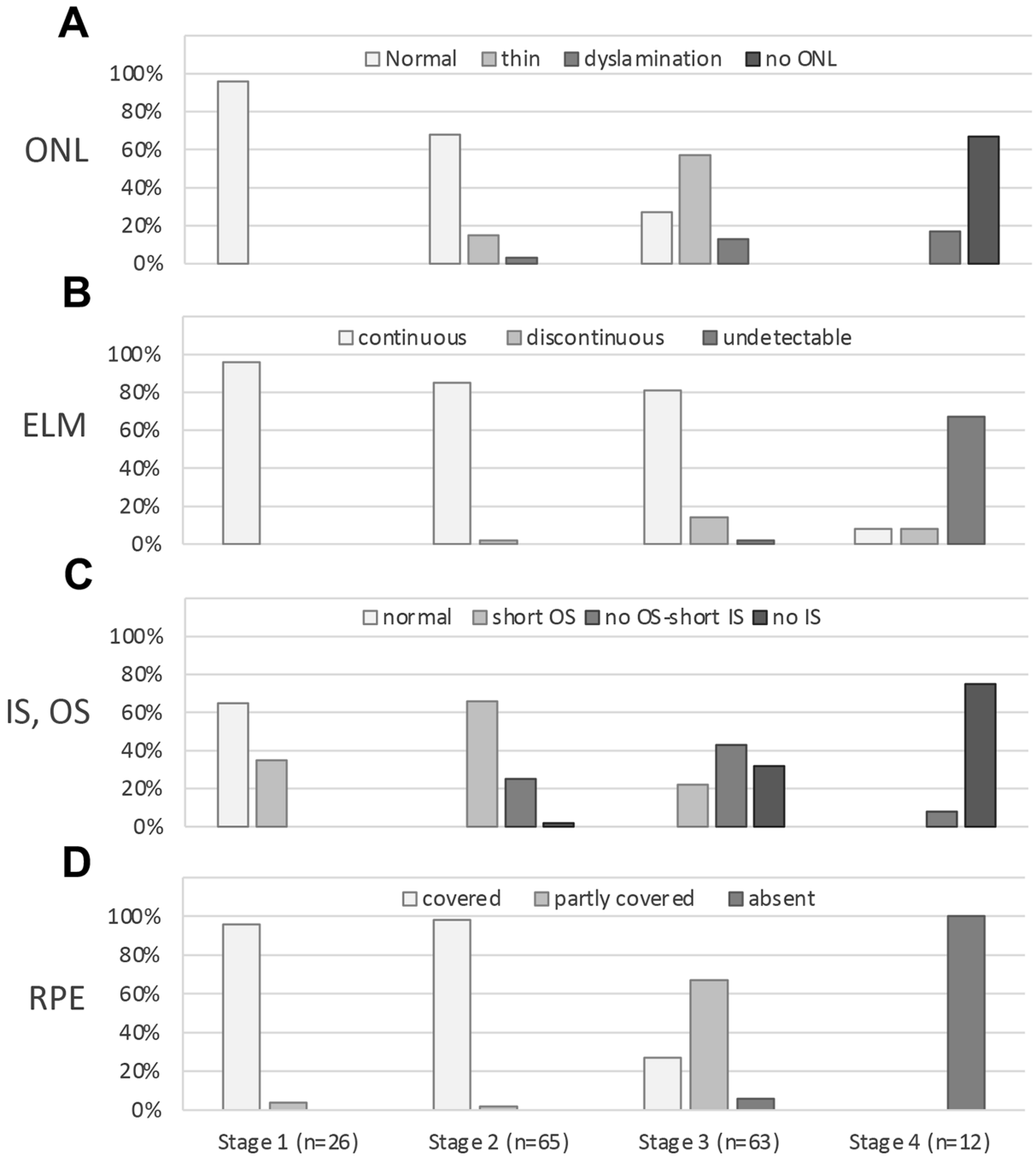

Figure 6. Outer retinal alterations above drusen at different FAF stages by histology.

A total of 166 drusen from both eyes were evaluated, which were assigned to 4 different stages based on clinical fundus autofluorescence (FAF) appearance. The number of drusen at each FAF stage as indicated under the graph on panel D applies to all graphs. **A.** Outer nuclear layer (ONL) morphology has 4 categories indicated by gray scale. Drusen at Stage 1 and 2 FAF tend to have a normal ONL (96% and 68%). Drusen at Stage 3 FAF tend to have a thin ONL (57%). Drusen at Stage 4 FAF tend to have no ONL (67%). ONL dyslamination can be observed above drusen with Stages 1–3 FAF and increase with severity. **B.** External

limiting membrane (ELM) morphology has 3 categories indicated by gray scale. Drusen at Stages 1–3 FAF tend to have a continuous ELM (96%, 85% and 81%), while drusen at Stage 4 FAF tend to have an undetectable ELM (67%). **C.** Inner segment (IS) and outer segment (OS) have 4 categories of morphology indicated by gray scale. Drusen at Stage 1 FAF tend to have a normal IS and OS (65%). Drusen at Stage 2 FAF tend to have a short OS (66%). Drusen at Stage 3 FAF tend to have no OS and a short IS (43%) or even no IS (32%); Drusen at Stage 4 FAF tend to have no IS or OS (75%). **D.** Retinal pigment epithelium (RPE) morphology has 3 categories indicated by gray scale. Drusen at Stage 1 and 2 FAF are completely covered by RPE (96% and 98%). Most drusen at Stage 3 FAF are partly covered by RPE (67%). All drusen with Stage 4 FAF lack RPE (100%). IS and OS were not evaluable above 9 drusen due to retinal detachment. ELM and ONL were not evaluable above 14 drusen due to retinal detachment.

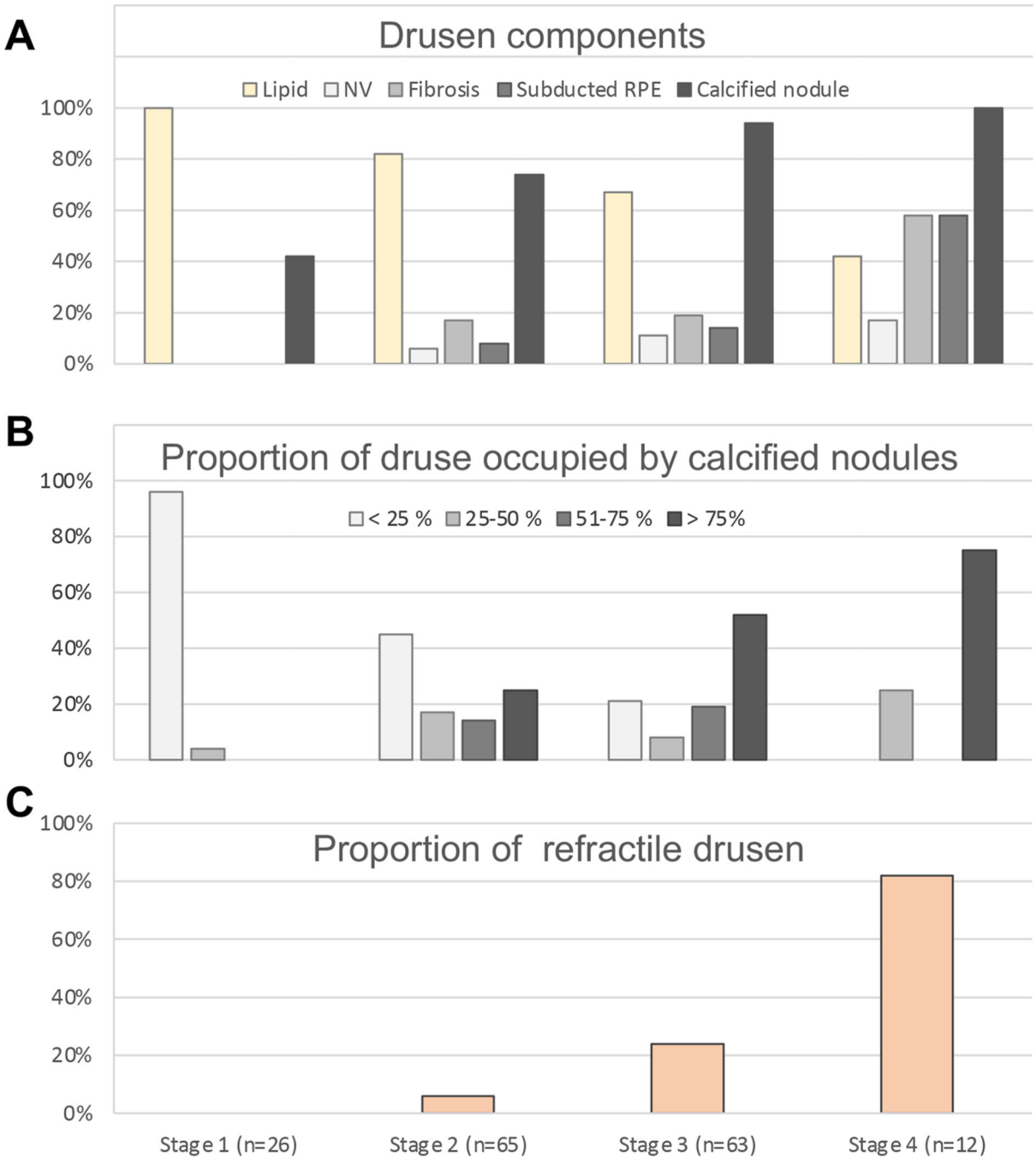

Figure 7. Drusen components by histology and drusen refractility on CFP at different FAF stages.

A total of 166 drusen from both eyes at different stages of clinical fundus autofluorescence (FAF) were evaluated. The number of drusen at each FAF stage is indicated under the graph on panel C and applies to all graphs. **A.** The percentage of drusen with lipid material (yellow) decreased with increasing FAF stages, while the percentage of drusen with neovascularization (NV), avascular fibrosis, subducted retinal pigment epithelium (RPE), or calcified nodule, indicated by gray scale, increased with increasing FAF stages. **B.**

Semi-quantitative analysis for calcified nodule, indicated by gray scale, shows that drusen in FAF Stage 1 and 2 tend to have smaller mass of calcified nodule (< 25%), while drusen in Stage 3 and Stage 4 tend to have larger mass (> 75%). **C.** Drusen refractility was evaluated based on color fundus photograph (CFP). Drusen in FAF Stage 4 (82 %) tend to be more refractile than drusen in FAF Stage 3 (24 %), Stage 2 (6 %) and Stage 1 (0 %).

Table 1.

Drusen at different FAF stages characterized by histology.

Drusen FAF Stages	Drusen height (μm)	Drusen width (μm)	BLamD (μm)	Drusen height +BLamD (μm)
Stage 1 (n=26)	25.1 ± 7.2	77.0 ± 33.3	4.6 ± 3.7	29.7 ± 9.5
Stage 2 (n=65)	43.9 ± 17.8	131.7 ± 61.0	7.5 ± 5.4	51.4 ± 20.0
Stage 3 (n=63)	66.7 ± 34.0	176.8 ± 90.4	12.6 ± 7.0	79.4 ± 37.4
Stage 4 (n=12)	68.5 ± 24.8	208.1 ± 80.6	6.7 ± 2.7	75.2 ± 26.3

FAF, fundus autofluorescence; BLamD, basal laminar deposit; Data are n and means ± SD. Drusen width is width at the base of drusen along the Bruch's membrane.